

FIRST RESULTS FROM CAR-TO-CAR AND CAR-TO-INFRASTRUCTURE RADIO CHANNEL MEASUREMENTS AT 5.2 GHz

Alexander Paier¹, Johan Karedal⁴, Nicolai Czik^{1,2}, Helmut Hofstetter³, Charlotte Dumard², Thomas Zemen², Fredrik Tufvesson⁴, Christoph F. Mecklenbräuer¹, Andreas F. Molisch^{4,5}

¹Institut für Nachrichtentechnik und Hochfrequenztechnik, Technische Universität Wien, Vienna, Austria

²Forschungszentrum Telekommunikation Wien (ftw.), Vienna, Austria

³mobikom austria AG, Vienna, Austria

⁴Dept. of Electric and Information Technology, Lund University, Lund, Sweden

⁵Mitsubishi Electric Research Labs, Cambridge, USA

apaier@nt.tuwien.ac.at

ABSTRACT

Car-to-car and car-to-infrastructure (henceforth called C2X) communications are constantly gaining importance for road-safety and other applications. In order to design efficient C2X systems, an understanding of realistic C2X propagation channels is required, but currently, only few measurements have been published. This paper presents a description of an extensive measurement campaign recently conducted in an urban scenario, a rural scenario, and on a highway. We focused on 4×4 multiple-input multiple-output (MIMO) measurements at a center frequency of 5.2 GHz with high Doppler resolution. As first results from evaluating the measurement data we present the power-delay profile and the delay-Doppler spectrum from a selected, especially interesting measurement run from an urban measurement route. We observe dispersed Doppler contributions between zero and the Doppler shift corresponding to the relative speed of the cars, and very concentrated (in the Doppler domain), contributions from double reflections. Surprisingly, we also found paths with larger delays and zero Doppler shifts.

I. INTRODUCTION

Traffic telematics applications are currently being intensely researched in order to make transportation safer and more efficient. One of the wireless transmission technologies for car-to-car and car-to-infrastructure, in the following called C2X, communications is the promising draft standard IEEE 802.11p which is currently under development [1]. In North America there is a frequency band allocated especially for this transmission technology at 5.9 GHz partitioned into seven 10 MHz channels.

For the efficient development and deployment of IEEE 802.11p and other C2X communication systems, many aspects of the C2X radio channel in the 5 GHz band are yet to be understood. Especially, the time-selective fading statistics of C2X communication links differ substantially from those of cellular communication networks. Currently, little is known about these statistics in the 5 GHz band. Furthermore, the characteristics of propagation channels for multiple-input multiple-output (MIMO) systems are completely unknown, even though MIMO is gaining more and more importance in the IEEE 802.11 standards [2].

Previous C2X channel measurement campaigns investigate only the car-to-car (C2C) case with cars driving in the same direction [3], [4], [5], [6]. However, we can anticipate (and our measurements confirm) that C2C with cars driving in opposite directions and car-to-infrastructure (C2I), will imply much higher Doppler shifts, because of higher relative speeds between transmitter and receiver. In [3] and [4], the radio channel is investigated at the lower frequency of 2.4 GHz, and [6] presents a narrow-band measurement campaign. Measured and simulated Doppler spectra for a frequency selective C2I channel are reported in [7]. In [8], C2I MIMO channel measurements are presented, but the focus is on path loss and not on Doppler spectra.

In order to alleviate the current lack of measurement data, we carried out a C2X radio channel measurement campaign in the 5 GHz band in Lund, Sweden. To the authors' knowledge these are the first wideband C2C radio channel measurements with a MIMO system in that band. Also novel is the high measurement bandwidth of 240 MHz, which leads to a high temporal resolution. The aim of these measurements is to investigate and analyze the joint spatio-temporal Doppler spectra. Three different scenarios, rural, highway, and urban, were investigated.

The remainder of the paper is organized as follows: Section II gives a detailed description of the measurement setup, including channel sounder, antennas, and environments. Section III describes first results from the urban environment. Section IV summarizes the paper and presents conclusions.

II. MEASUREMENTS

A. Measurement equipment

1) Channel sounder

The measurements were done with the RUSK LUND channel sounder that performs MIMO measurements based on the "switched-array" principle [9]. In this measurement campaign we used a center frequency of 5.2 GHz. This choice of measurement frequency was dictated by regulatory concerns, as well as by the availability of antenna arrays. This band is close enough to the 5.9 GHz band such that no significant differences in propagation characteristics is to be anticipated. Using the RUSK LUND channel sounder we were able to use a very high measurement bandwidth of 240 MHz, which results in an intrinsic delay resolution of $\Delta\tau = 4.2$ ns. The test signal length,

also called maximum delay, was set to $3.2 \mu\text{s}$, which is equal to a maximum propagation path length of 959 m. For the measurements we used the maximum transmit power of 27 dBm.

In this measurement campaign we focus on time-variant channels. To achieve a high Doppler resolution, we had to choose the snapshot repetition rate properly. The snapshot time, i.e. the time over all $P = 16$ temporal multiplexed channels, is equal to $2 \times 4 \times 4 \times 3.2 = 102.4 \mu\text{s}$, where the factor 2 stems from the guard interval between consecutive snapshots used by the sounder. To obtain feasible file sizes but still allow for sufficient measurement time and high Doppler resolution, we set the snapshot repetition rate to $t_{\text{rep}} = 307.2 \mu\text{s}$. Using $N = 32500$ snapshots, we could continuously measure for 10 s recording a file of 1 GB for each measurement. The maximum Doppler shift for a time invariant channel can be calculated with

$$\nu_{\text{max}} = \frac{1}{2 \cdot t_{\text{rep}}}. \quad (1)$$

With these settings, the maximum resolvable Doppler shift is equal to 1.6 kHz, which corresponds to a maximum speed of 338 km/h. For the scenarios presented in this paper, the relative speed between the two cars was 100 km/h maximum, therefore we can resolve 3.4-fold Doppler frequencies (e.g. originating from double reflections).

From the channel transfer functions measured by the channel sounder, we obtain, by means of an inverse Fourier transform, using a Hanning windowing function, the complex channel impulse responses (IRs)

$$h(nt_{\text{rep}}, k\Delta\tau, p). \quad (2)$$

These IRs were imported as matrices into Matlab with an overall array size of $32500 \times 769 \times 16$ ($N \times K \times P$). For calculations in Matlab, only parts of these matrices were used, because of working memory limitations. In (2), n is the time index, from 0 to $N - 1$, k is the delay index, from 0 to $K - 1$, and p is the channel number, from 1 to P .

2) Antennas

On both link ends we used elements from uniform circular arrays of microstrip antennas. Each array consists of a circle (the Rx array consists of 4 circles) of 16 dual-polarized elements, from which we selected 4 symmetrically placed, vertically polarized elements. With the reference bearing 0° (as seen from a top view of the arrays) being in the direction of driving, the selected antenna elements were directed at 45° , 135° , 225° , and 315° . The directions of the main lobes of these elements were the same for both measurement cars and are described in Fig. 1. Each antenna array was mounted on top of a stack of Euro pallets, which, when mounted on the car's platform, provided a total antenna height of 2.4 m above the ground (see Fig. 4).

3) Route documentation

To document the routes and scenarios during the measurements (traffic, weather, environment) we used two video cameras. Each camera was equipped with a fisheye lens, in order to capture a field of view of about 150° . One camera was placed in

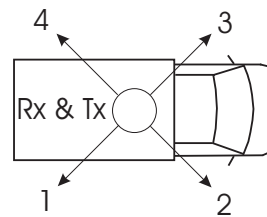


Figure 1: Direction of the main lobes of each antenna element for receiver and transmitter



Figure 2: Laser distance meter and video camera for documentation

the passenger compartment of the car containing the transmitter. The other camera was mounted in the back of the receiver (Rx) transporter, where the car's tarpaulin was opened at the back.

Global Positioning System (GPS) position data was directly available from the transmitter and receiver of the channel sounder at a rate of one position sample per second. Moreover, we used one additional GPS system in order to record the actual speed of the transmitter (Tx) car. This GPS system also provided a real-time display of the actual car position.

In order to obtain a more accurate measurement of the distance between the cars, we also used a laser distance meter LD90-3100HS from Riegler Laser Measurement Systems GmbH. It was programmed such that it supplied the actual distance every 100 ms (and in some measurements every 200 ms). Fig. 2 shows the laser distance meter and one of the video cameras, which were mounted together on a monopod.

B. Cars

We used two transporters (similar to pickup trucks), of the same type, see Fig. 3. The loading platform of the transporters were covered with a plastic tarpaulin to protect the measurement equipment and antennas against air stream (and possible rain), thus providing greater stability for the antennas. Since the height of the tarpaulin cover is larger than the driver's cabin, the antennas could be mounted on the loading platform in such a way that they could "see" over the driver's cabin (though we cannot exclude the possibility that waves reflected from the road, and thus arriving from an elevation angle smaller than 0 degree, might have been attenuated by the driver's cabin). Fig. 4 presents the measurement cars containing the channel



Figure 3: Measurement car



Figure 4: Loading spaces with the measurement equipment — left Rx, right Tx

sounders, batteries, and antennas placed on the loading space.¹

C. Measurement practice

The measurement campaign was conducted during three days, and a total of 141 measurement runs were recorded.

In the Rx car, one person acted as driver, another one controlled the channel sounder, and the third person wrote the measurement protocol.

The Tx car was steered by one driver, another person controlled the additional GPS-system and the laser distance meter with a laptop. The third person was responsible for the video documentation and pointing the laser distance meter onto the Rx car using a telescope.

The laser distance meter was only used for C2C measurements in same direction. In this case the Tx car followed the Rx car. Consequently it was also possible to hold approximately the same distance between the cars during the measurement runs.

Communication between the two cars was handled through walkie-talkies operating at a frequency of 446 MHz.

D. Measurement scenarios

Three different scenarios, rural, highway, and urban, were measured.

In each scenario, see Fig. 6, we carried out two kinds of C2C measurements: with the two measurement cars driving in (i) the same, and (ii) opposite directions. Car speed and the

¹battery lifetime of the Rx equipment was extended by means of a petrol-driven power generator, which was also mounted on the loading space.



Figure 5: Photo of the street “Esplanaden” in the center of Lund

distance between the cars was varied between different measurement runs in the range of 30 – 110 km/h and 30 – 130 m, respectively. In the highway scenario, we also carried out C2I measurements, where the transmitter was placed on a bridge above the road.

This paper only presents results from a measurement of the urban scenario, which was performed in the city center of Lund, a medium-sized Swedish city. The city center of Lund is characterized by four-story buildings, and is therefore “urban” in the sense of many European cities, but definitely not “metropolitan”.

Weather conditions during the measurements ranged from sunny to heavy rain and hail.

III. EVALUATION RESULTS

In this section we present first evaluation results from a selected, especially interesting urban C2C opposite-direction measurement. The cars were traveling at a speed of 50 km/h, each. Fig. 5 presents the measured street having buildings on the left hand side and leafless trees on the right hand side.

A. Power-delay profile

In the considered measurement the two cars were driving in opposite directions and were passing each other after 1.6 s of the 10 s measurement time. The power-delay profile (PDP), Fig. 7, was calculated by averaging the magnitude squared over 40 wavelengths, in order to average over the small scale fading, and taking the sum over all 16 channels

$$P_{\text{PDP}}(it_{\text{av}}, k\Delta\tau) = \frac{1}{L} \sum_{n=iL}^{(i+1)L-1} \sum_{p=1}^P |h(nt_{\text{rep}}, k\Delta\tau, p)|^2. \quad (3)$$

This equals at a relative speed of 100 km/h a distance of 2.3 m and thus yields an averaging time of $t_{\text{av}} = 83$ ms, i.e. $L = 271$ snapshots. Fig. 7 shows the strong line of sight (LOS) path with decreasing delay until 1.6 s (cars passing) and increasing delay afterwards. There are also several paths with constant delay over the time. The most likely explanation for such a constant-delay path is depicted in Fig. 8. The reflector is along a straight line connecting the two cars, where one car is approaching the reflector and the other is driving away from it. Note that such paths should also show zero Doppler shift. For the further calculations only one MIMO channel was chosen. Additionally,



Figure 6: Satellite photo of (a) the rural scenario in the north-east of Lund, (b) the highway E22 in the east of Lund, (c) the urban scenario with the measurement route on the street “Esplanaden” in the center of Lund

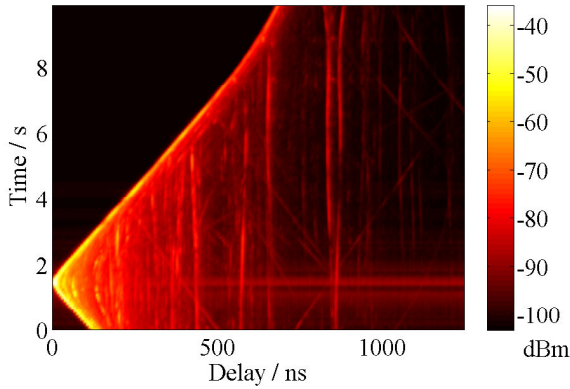


Figure 7: Average power delay profile

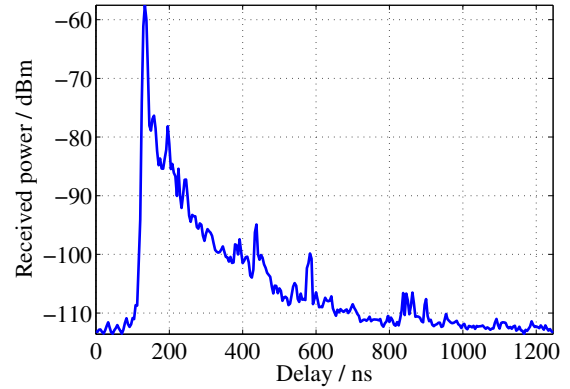


Figure 9: Average power-delay profile at $t = 3$ s

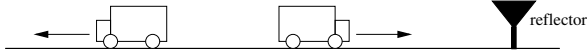


Figure 8: Scenario leading to constant delay reflectors

we present the average PDP after a time of $t = 3$ s, corresponding to a distance between the cars of 41 m. After selecting the corresponding snapshots $n_1 = 9769$ and $n_2 = 10039$ from the data, the average PDP is calculated as

$$P_{\text{PDP}}(k\Delta\tau) = \frac{1}{n_2 - n_1 + 1} \sum_{n=n_1}^{n_2} |h(nt_{\text{rep}}, k\Delta\tau, 1)|^2. \quad (4)$$

Fig. 9 shows the calculated logarithmic average PDP for channel $p = 1$ (Tx antenna element 1, Rx antenna element 1), which is one of the four channels, where the main lobes of the antennas were facing towards each other after the cars have passed by.

The multipath component corresponding to the LOS path arrives after a delay of $\tau = 138$ ns, i.e. 41 m, which is the distance between the two cars. We also observe several more paths arriving until a delay of $\tau = 1200$ ns. In the following we will discuss the impulse at $\tau = 433$ ns in more detail. Evaluations

showed that this path exhibits a constant delay during the measurement run from $t = 0$ s to approximate $t = 6$ s, see Fig 7.

B. Delay-Doppler spectrum

We calculated the short-time delay-Doppler spectrum

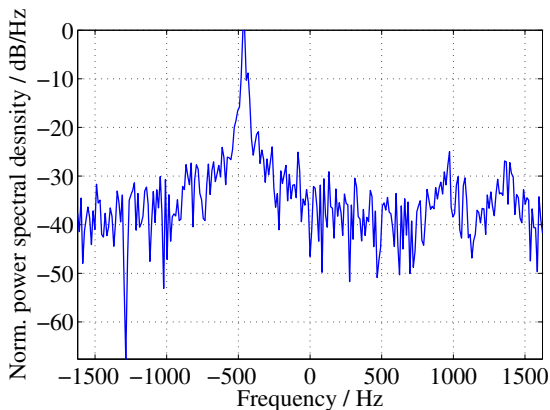
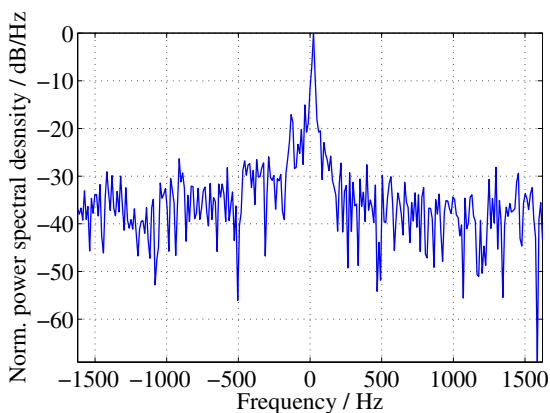
$$p_{\text{DD}}(r\Delta\nu, k\Delta\tau) = f_{\text{fit}}(h(nt_{\text{rep}}, k\Delta\tau, 1)), \quad (5)$$

for the same data as before, using the fast-Fourier transformation over 271 snapshots which results in a Doppler resolution of $\Delta\nu = 12$ Hz, for $-135 \leq r \leq 135$. We observe dispersed contributions between -500 Hz and 0 Hz, but also paths from obvious double reflections at -900 Hz and $+500$ Hz. Fig. 10 and Fig. 11 show the logarithmic normalized power spectral densities over the Doppler frequency

$$P_{\text{DD, norm}}(r\Delta\nu, k\Delta\tau) = \frac{|p_{\text{DD}}(r\Delta\nu, k\Delta\tau)|^2}{|p_{\text{DD}}(r\Delta\nu, k\Delta\tau)|_{\text{max}}^2} \quad (6)$$

for the two peaks: (i) the LOS path at a delay of $\tau = 138$ ns and (ii) the constant-delay path at $\tau = 433$ ns, both at the time of $t = 3$ s.

The Doppler spectrum of the LOS path in Fig. 10 shows a peak at -469 Hz, corresponding to a relative speed of 97 km/h

Figure 10: Doppler profile at delay-tap $k = 33$ (138 ns)Figure 11: Doppler profile at delay-tap $k = 104$ (433 ns)

between Tx and Rx, which agrees very well with the intended 100 km/h. Negative Doppler frequencies indicate that the cars are separating.

The Doppler spectrum of the constant-delay path in Fig. 11 shows a peak at a frequency of 24 Hz, i.e. a relative speed of 5 km/h, which we can effectively treat as zero Doppler. Note that this finding is congruent with our deductions in Section A. Indeed, the videos of this scenario indicate that the reflector is most likely a traffic sign located in the middle of the street in front of the Tx car. With an approximate size of 400 mm the traffic sign is a good reflector at our wavelength of 5.8 mm.

IV. CONCLUSIONS

We presented a detailed description of our car-to-car and car-to-infrastructure (C2X) measurement campaign in the city of Lund using the RUSK LUND channel sounder at a center frequency of 5.2 GHz. We measured in three different scenarios (rural, highway, urban). The measurements allowed for a high Doppler resolution and a maximum Doppler shift of 1.6 kHz in a 4×4 MIMO system. The focus of this work was to show the Doppler spectrum in a typical traffic situation in the urban scenario. The paper presents first results of evaluating car-to-car (C2C) channels, with the cars driving in opposite directions, each with 50 km/h.

We found that the paths are dispersed in the Doppler domain between 0 Hz and the Doppler corresponding to the relative speed of the cars. Additionally, we observed double reflections causing Doppler contributions with twice the frequencies. We also found several paths with a constant delay and zero Doppler over time. Such a path is caused by a reflector located in the straight line of driving, where one car is approaching the reflector whereas the other is driving away from it. We found these reflectors to be most likely traffic signs, which reflects strongly in the measured frequency band.

After these promising first results, we will further analyze the measurements in order to gain a deeper insight into the significant propagation effects of C2X communications.

V. ACKNOWLEDGMENTS

This work was carried out with partial funding from Kplus and the Wiener Wissenschafts- Forschungs- und Technologiefonds (WWTF) in the ftw. project I0 and I2 – “Math+MIMO”. The authors would like to thank RIEGL Laser Measurement Systems GmbH and MEDAV GmbH for their generous support.

REFERENCES

- [1] “Draft amendment to wireless LAN medium access control (MAC) and physical layer (PHY) specifications: Wireless access in vehicular environments,” IEEE P802.11p^m/D2.01, March 2007.
- [2] “Draft amendment to wireless LAN medium access control (MAC) and physical layer (PHY) specifications: Enhancements for higher throughput,” IEEE 802.11n D1.0, March 2006.
- [3] G. Acosta, K. Tokuda, and M. A. Ingram, “Measured joint doppler-delay power profiles for vehicle-to-vehicle communications at 2.4 GHz,” in *Global Telecommunications Conference 2004*, 29 November – 3 December 2004.
- [4] G. Acosta and M. A. Ingram, “Model development for the wide-band expressway vehicle-to-vehicle 2.4 GHz channel,” in *IEEE Wireless Communications and Networking Conference (WCNC) 2006*, 3–6 April 2006.
- [5] G. Acosta-Marum and M. A. Ingram, “Doubly selective vehicle-to-vehicle channel measurements and modeling at 5.9 GHz,” in *Wireless Personal Multimedia Communications (WPMC) 2006*, 17–20 September 2006.
- [6] J. Maurer, T. Fügen, and W. Wiesbeck, “Narrow-band measurement and analysis of the inter-vehicle transmission channel at 5.2 GHz,” in *Vehicular Technology Conference (VTC) 2002*, 6–9 May 2002.
- [7] X. Zhao, J. Kivinen, P. Vainikainen, and K. Skog, “Characterization of doppler spectra for mobile communications at 5.3 GHz,” in *IEEE Transaction on Vehicular Technology*, January 2003.
- [8] C. Schneider, A. Hong, G. Sommerkorn, M. Milojevic, and R. S. Thomä, “Path loss and wideband channel model parameters for WINNER link and system level evaluation,” in *Third International Symposium on Wireless Communication Systems (ISWCS) 2006*, 5 – 8 September 2006.
- [9] R. Thomä, D. Hampicke, A. Richter, G. Sommerkorn, A. Schneider, U. Trautwein, and W. Wirtzner, “Identification of time-variant directional mobile radio channels,” *IEEE Trans. on Instrumentation and measurement*, vol. 49, pp. 357–364, 2000.